# Variability of aerosol optical depth and recent recessional trend in Dokriani Glacier, Bhagirathi Valley, Garhwal Himalaya

**Sanat Kumar Das[1,3,*], D. P. Dobhal[2] and N. Juyal[1]**

[1]Physical Research Laboratory, Navrangpura, Ahmedabad 380 009, India
[2]Wadia Institute of Himalayan Geology, GM Road, Dehra Dun 248 001, India
[3]Present address: National Atmospheric Research Laboratory, Gadanki, Tirupati 517 502, India

**Temporal changes in aerosol optical depth (AOD) during 2001–2008 obtained from Moderate Resolution Imaging Spectroradiometer on-board Terra satellite and the glacier recession data of Dokriani glacier in the Bhagirathi valley show a reasonable correlation ($R^2 = 0.86$). An increase in AOD was observed after 2005, which coincides with the accelerated recession of the Dokriani glacier. We hypothesize that increased AOD over the Himalayan region led to enhanced aerosol heating, which contributed to the recent observed recessional trend of the glacier. This suggests that AOD can be used to obtain the spatial and temporal changes in microclimatic conditions in the inaccessible glaciated terrain of the Himalayas.**

**Keywords:** Aerosol optical depth, climate variability, glacier, Himalayas, recession, satellite.

GLACIERS are the natural sensors of climate variability and provide a visible expression of climate change. Studies have shown that Himalayan glaciers have responded to both long ($\sim 10^4$) and short-term ($< 10^3$ years) climatic fluctuations caused due to natural forcing factors during the Late Quaternary period[1–3]. However, in recent times there are concerns that anthropogenically-induced increase in greenhouse gases (GHGs) and aerosols may accelerate melting of the Himalayan glaciers[4]. This would negatively affect water supply in the next few decades in India, including China and part of Asia, also known as the Himalaya–Hindu Kush region[5]. According to the IPCC Report 2007 (ref. 6), most mountain glaciers and ice caps have been shrinking with the frontal retreat probably having started about 1850. It has been further suggested that climate change will affect the magnitude of accumulation and ablation, and the length of the mass balance seasons. In such a scenario, the worst affected would be the small Himalayan glaciers. The reason being that small glaciers have virtually no response time lag (only a few years) between climate variability and glacier response[7]. In recent times, there has been growing concern over warming caused due to the increase in GHGs such as carbon dioxide and methane, and aerosols like soot (black carbon). In terms of direct radiative forcing, studies have suggested that soot may be the second most important component of global warming, after carbon dioxide[8]. Soot is anthropogenic in origin (combustion of biomass and fossil fuels); compared to this, mineral aerosols are naturally occurring continental dust from dryland areas which are transported by the winds[9–11]. There are evidences to suggest that air-temperature trend over the Himalayan region has accelerated (between 0.15 and 0.3 K/decade) during the past several decades[4,12]. Unlike soot, the mineral aerosols are considered to have a negative forcing near the Earth's surface due to backscattering of solar irradiance. However, the same aerosols in the lower and middle troposphere (6–8 km) are observed to be associated with warming[5]. A majority of the Himalayan glaciers are located above 4000 m asl.

In this communication, an attempt has been made to observe if there exists any correlation between the recession of the Dokriani glacier and the temporal changes in aerosol concentration using aerosol optical depth (AOD) variation. The Dokriani glacier (Figure 1 *a*) in the Bhagirathi valley has one of the longest documentations of recessional history (1962–2007) and the actual mass balance data are available since 1991 (ref. 13). The study was motivated by the following reasons. (i) The Himalayas together with the Tibetan plateau have the highest concentration of glaciers outside the polar region; thus the region provides a unique opportunity to study the impact of aerosols, if any, on glacier recession (melting). (ii) Recent studies have shown that the foothills of the Himalayas, viz. the Indo-Gangetic Basin (IGB) is one of the major sources of anthropogenic aerosols in the region[14–18]. In addition, the Great Indian Desert (Thar Desert) in western India produces significant amount of aerosol dust which is transported by the pre-monsoon (March–May) winds to the IGB[9–11]. (iii) There are studies to suggest that a mixture of locally produced anthropogenic aerosol (soot) with natural aerosol (dust) produces strong atmospheric warming over the IGB[11].

The present study was carried out in the medium-sized Dokriani glacier (lat. 30°49′–30°52′N and long. 78°47′–78°51′E) in the Bhagirathi river basin (Upper Ganga river basin) in Garhwal Himalaya (Figure 1 *a*). The Dokriani glacier originates from the Draupadi ka Danda group of peaks at an elevation of 6000 m asl and is joined by two cirque glaciers (Figure 1 *a*). The glacier follows NNW direction for about 2 km, before it turns towards WSW and terminates at an altitude of 3915 m (as on 2008). The length of the glacier is 5.5 km, with its width varying from 0.08 to 2.5 km. The total catchment area is 15.7 km$^2$, with glacier ice covering an area of 7.0 km$^2$. The thickness of the glacier ice varies from 25 to 120 m between snout and accumulation zone[19]. The lower reaches of the ablation

*For correspondence. (e-mail: sanatkrdas@gmail.com)

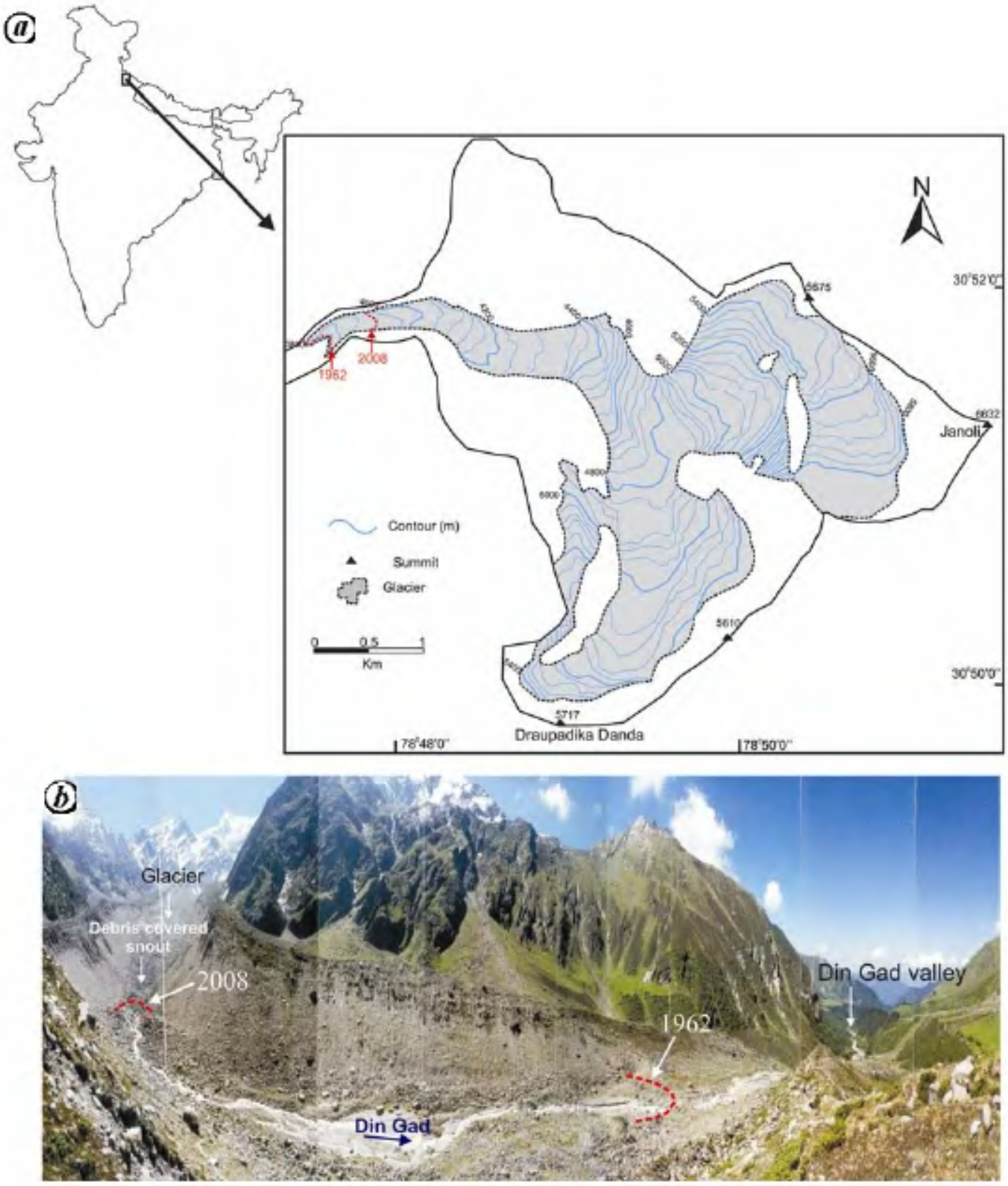


**Figure 1.** ***a***, Map of Dokriani glacier catchment showing morphology of the glacier; drawn from 1962 and 1995 Survey of India Topographic map. Snout during 1962 and 2008 is marked by red dashed lines. ***b***, Field photograph of Dokriani glacier. Snout position during 1962 and 2008 is marked by red dashed lines.

zone are covered by debris (Figure 1 *b*). The melt-water stream emerging from the glacier is known as Din Gad and joins River Bhagirathi at Bhukki[13].

Although continuous snout-monitoring data exist since 1991, in this study we have considered the recessional data obtained from 2001 to 2008, because the AOD data are available only from 2001 onwards. Snout-retreat data indicate that during the above period, glacier recession rate was 15.5 m/year and the mean temperature fluctuations recorded were 3–4.8°C during 2001–2007 at the glacier basin[20].

Satellite-derived AOD is a cost-effective way to monitor and study aerosol distribution globally. Monthly average Moderate Resolution Imaging Spectroradiometer (MODIS) AOD has been used to study AOD distribution in the spatio-temporal domain over the Indian subcontinent since 2001 (ref. 21). As mentioned earlier, mineral aerosols increase scattering and cloud cover, and re-radiation of solar energy to space (negative forcing)[5]. However, in the lower and middle troposphere they have positive forcing effect (warming)[22–24]. In view of this, the presence of mineral aerosols in the lower and middle troposphere may enhance the direct temperature forcing that in turn would assist the melting of the glaciers in the Himalaya[5].

Since aerosols attenuate the solar flux received at the Earth's surface by scattering and absorbing, to estimate the solar flux attenuation, one needs to know the aerosol loading which can be estimated using AOD values for a given period/year. Higher AOD represents higher solar energy attenuation in the atmosphere and results in higher amount of solar energy stored by the atmosphere. AOD (at 0.550 μm) around the Dokriani glacier (long. 78–79°E and lat. 30–31°N) was obtained using Level-3 MODIS[25,26] gridded atmosphere daily global product 'MOD08_D3'. Daily retrieved (AOD) MOD08_D3 product files are available in Hierarchical Data Format (HDF-EOS) at a spatial resolution of 1° by 1°.

The rate of change of temperature ($\mathrm{d}T/\mathrm{d}t$) in an atmospheric layer due to radiative heating is called radiative heating rate (units = K/day), and is defined as

$$\frac{\mathrm{d}T}{\mathrm{d}t} = -\frac{1}{\rho C_p}\frac{\mathrm{d}F}{\mathrm{d}Z}, \qquad (1)$$

where $C_p$ is the specific heat capacity, $\rho$ is the density of air and $\mathrm{d}F/\mathrm{d}Z$ is the change in radiative flux within the atmospheric layer of height $Z$ and $Z + \mathrm{d}Z$. Differences in heating rates with and without aerosols were computed. Atmospheric radiative transfer code (SBDART) developed at the University of California, Santa Barbara[27], was used to estimate aerosol heating rate over the study area. SBDART is a software tool that computes plane-parallel radiative transfer in clear and cloudy conditions. All important processes that affect the ultraviolet, visible and infrared radiation fields are included. The present study computes the aerosol heating rate for clear-sky conditions.

It is further suggested that aerosol-induced atmospheric heating is a function of the absorption properties of the aerosols present in the atmosphere[28]. For example, soot has the property of strong absorption of solar radiation in the lower atmosphere and is usually found in confined surroundings (in and near the source regions and within the boundary layer). However, if there is assistance provided by thermal convection due to enhancement of surface temperature, the soot particles can reach higher altitudes[29]. Recent studies have demonstrated that the foothill region of the Himalayas, viz. the IGB is one of the largest sources of soot particles that are generated due to fossil fuel and biomass burning[14–18]. Similarly, dust can also act as a potential solar absorber. It has been suggested that significant solar radiation can be absorbed by dust that originates from the Thar Desert during pre-monsoon[24]. This dust is eventually transported into the Himalayan region by pre-monsoonal winds[10] and may assist in the warming of the Himalayan region.

To compute aerosol heating rate, the radiative transfer model requires Angström exponent, single scattering albedo (SSA) and asymmetry parameter ($g$). The Angström exponent provides information about the aerosol size distribution from the spectral information of aerosol optical properties obtained from MODIS observations. Other two parameters are calculated using the optical properties of aerosols and clouds (OPAC) model[30]. Knowledge of aerosol chemical components over the Himalayan and the foothill region (IGB), is important in order to obtain aerosol optical properties using the OPAC model[18]. Towards this, we used the published data[11,18,28,31]. In the calculation of heating rate, a major uncertainty arises due to the Angström exponent and SSA. The modelled Angström exponent is 1.2, which is close to the value obtained by MODIS. We observed that the Angström exponent has a seasonal variation of about 25% over the Dokriani glacier, which causes about 5% uncertainty in the estimated heating rate. The modelled SSA and $g$ at 0.55 μm are 0.91 and 0.70 respectively. The uncertainty introduced by $g$ is less than 1%. Comparing the modelled SSA values with published values from the limited Himalayan stations shows a variation between 0.78 and 0.90 (refs 28, 31).

Surface reflectance is also an important parameter in estimating the aerosol heating rate. In the present study, 8-days MODIS surface reflectance of 500 m resolution at seven wavelengths centred at 0.47, 0.56, 0.65, 0.86, 1.24, 1.64 and 2.13 μm were used. Due to unavailability of the measured vertical distribution of temperature and relative humidity from the study area, the data available from the tropical atmosphere were used.

Estimation of aerosol-induced heating also requires aerosol vertical profile, which provides information about total aerosol loading and aerosol layer height. We obtained the aerosol vertical profile from the space-borne lidar Cloud-Aerosol Lidar with Orthogonal Polarization (CALIOP) on-board Cloud-Aerosol Lidar with Orthogonal Polarization Satellite Observation (CALIPSO) satellite. CALIOP observes aerosol loading vertically and horizontally at a high spatial resolution along the satellite track. From the surface to 8 km, the vertical resolution is 30 m and the nominal horizontal resolution is 1/3 km (refs 32, 33). CALIPSO satellite was launched in April 2006 and hence we used the mean seasonal vertical distributions of aerosol during 2007–2008 for the entire calculation. Figures 2 *a* and *b* represent the overpass of the CALIPSO satellite in the study area (shaded region) on 27 May and 26 December 2007 respectively. Figures 2 *c* and *d* show the backscattered attenuated (scattered + absorbed) signal (at 0.532 μm) observed by the satellite along the track, and Figures 2 *e* and *f* show the measured aerosol vertical profiles. It can be seen from Figure 2 *c* that during May, aerosols reach up to a height of 6 km, whereas during December they are confined to around 3 km (Figure 2 *d*). The heating rate, therefore, is calculated within the lower atmosphere (up to 6.0 km). Thicker vertical profile during summer is due to higher surface temperature, which in turn leads to high boundary layer and thereby facilitates the upward movement of soot aerosols. Additionally, during summer frequent dust storms over the Thar Desert are a common phenomenon.

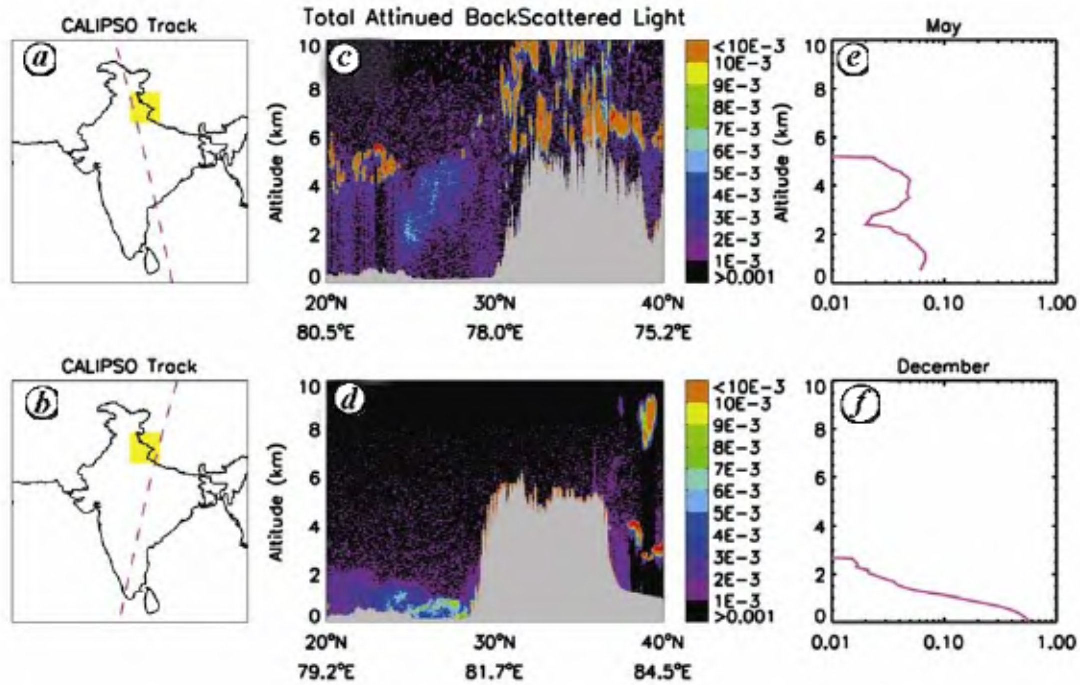


**Figure 2.** *a*, *b*, Satellite track. *c*, *d*, Profiles of 0.532 μm backscatter return signal ($km^{-1}$ $sr^{-1}$) from the CALIPSO lidar. *e*, *f*, Vertical distribution of aerosols over the study area during 27 May and 26 December 2007 respectively.

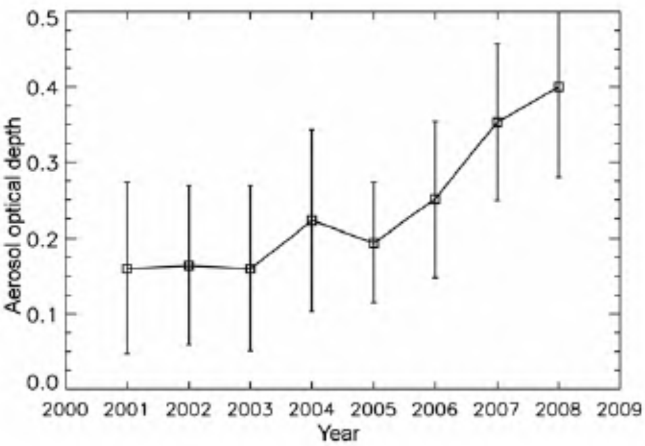


**Figure 3.** Variation in annual mean aerosol optical depth (AOD) between 2001 and 2008. Vertical bars represent variation around the yearly mean. Note an appreciable increase after 2005.

Satellite observations suggest that the dust aerosols are transported northeastward into the IGB and further northward into the higher Himalayan mountains[10,11]. The averaged aerosol vertical profile considered can introduce an uncertainty of about 5% in the calculation of aerosol heating rate.

Similarly, the annual mean AOD is obtained from the monthly mean AOD for a particular year and the corresponding annual mean aerosol heating rate is computed for that year. However, there is a large seasonal variation of yearly AOD (Figure 3) which is also included in this calculation. Since the AOD increases during summer and decreases during winter, it reflects as the maximum and minimum aerosol heating rate calculated for that particular year. The difference between these two extreme values gives the variation of the mean heating rate within that year.

Annual mean variation of AOD shows a near constant value centred around 0.15–0.2 during 2001–2005, followed by a steady increase till 2008 (Figure 3). Further, we observed a strong intra-annual variation in the monthly mean AOD, which reaches a maximum value during the pre-monsoon season (March–May) and decreases significantly during winter season (November–February). This is in agreement with the results obtained by earlier workers[34].

The higher aerosol loading like soot and dust during summer can cause significant atmospheric heating, which has a large impact on regional climate change[11]. The atmospheric heating rate induced by aerosol loading over the study area, computed using the aerosol transfer model is shown in Figure 4. Vertical bars represent the uncertainty of the estimated values caused due to the intra-annual variation of aerosols (type and concentration). The estimated heating rate based on the temporal changes in AOD ranges from 0.4 K/day (2001) to 1.2 K/day (2008). The trend of estimated heating rate compares well with that observed at the glacier[20]. Similarly, a close correspondence between the pattern of AOD variation and glacier recession also has been observed (Figure 5). Both show an appreciable increase after 2005, implying that AOD-induced temperature changes could have contributed towards the accelerated recession of the Dokriani glacier. It would be worth exploring the causes for a sudden increase in aerosol concentration in the study area after 2005.

Studies based on aerosols have suggested that if the pattern of increase continues, the future of the Himalayan glaciers is not encouraging. For example, there has been a positive feedback (radiative forcing) caused due to the brown cloud along with that of the anthropogenic GHGs. This has caused a combined warming trend of 0.25 K/decade[5,35], which according to Ramanathan *et al.*[4] is sufficient to account for the observed retreat of the Himalayan glaciers.

The present study is preliminary in nature. Nevertheless, a close correspondence between the temporal increase in AOD and glacier recession data based on real-time snout recession measurement suggests that along with other proxies, AOD also can be used effectively in the Himalayan glacier studies. We suggest that it is important

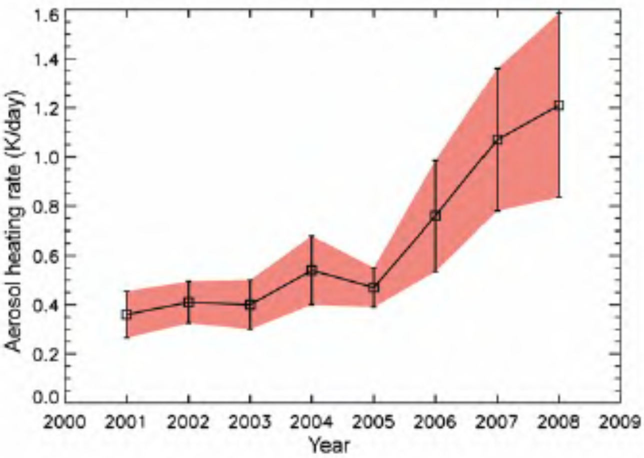


**Figure 4.** Annual mean aerosol heating rate calculated based on annual mean AOD suggests an increase from 0.4 K/day during 2001 to around 1.2 K/day during 2008.

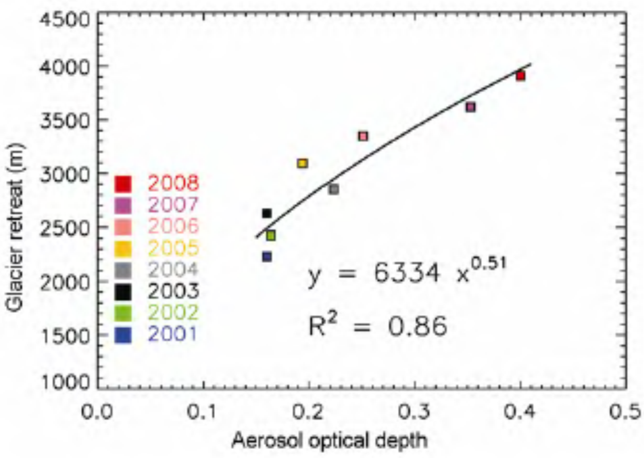


**Figure 5.** Correlation between AOD and cumulative recession rate of the Dokriani glacier between 2001 and 2008.

to have *in situ* aerosol measurements in key glacier sites supported by satellite remote sensing data. This would help us in understanding the current status and the future trends of the Himalayan glaciers in a better way.


1. Sharma, M. C. and Owen, L. A., Quaternary glacial history of the Garhwal Himalaya, India. *Quat. Sci. Rev.*, 1996, **15**, 335–365.
2. Pant, R. K., Juyal, N., Basavaiah, N. and Singhvi, A. K., Late Quaternary glaciation and seismicity in the Higher Central Himalaya: evidence from Shalang basin (Goriganga), Uttaranchal. *Curr. Sci.*, 2006, **90**, 1500–1505.
3. Nainwal, H. C., Chaudhary, M., Rana, N., Negi, B., Negi, R. S., Juyal, N. and Singhvi, A. K., Chronology of the Late Quaternary glaciation around Badrinath (upper Alaknanda Basin): preliminary observations. *Curr. Sci.*, 2007, **93**(1), 90–93.
4. Ramanathan, V., Ramana, M. V., Roberts, G., Kim, D., Corrigan, C., Chung, C. and Winker, D., Warming trends in Asia amplified by brown cloud solar absorption. *Nature*, 2007, **448**, 575–578.
5. Barnett, T. P., Adam, J. C. and Lettenmaier, D., Potential impact of a warming climate on water availability in snow-dominated regions. *Nature*, 2005, **438**, 303–309.
6. Lemke, P. *et al.*, Observations: changes in snow, ice and frozen ground. In Climate Change 2007: The Physical Science Basis. Contribution of Working Group I to the Fourth Assessment Report of the Intergovernmental Panel on Climate Change, New York, Cambridge University Press, UK, 2007.
7. Kaser, G., Juen, I., Georges, C. and Tamayo, J. G., The impact of glaciers on the runoff and the reconstruction of mass balance history from hydrological data in the tropical Cordillera Blanca, Peru. *J. Hydrol.*, 2003, **282**, 130–144.
8. Jacobson, M. Z., Strong radiative heating due to the mixing state of black carbon in atmospheric aerosols. *Nature*, 2001, **409**, 695–697.
9. Dey, S., Tripathi, S. N., Singh, R. P. and Holben, B. N., Influence of dust storms on the aerosol optical properties over the Indo-Gangetic basin. *J. Geophys. Res.*, 2004, **109**, D20211.
10. Hedge, P., Pant, P., Naja, M., Dumka, U. C. and Sagar, R., South Asian dust episode in June 2006: aerosol observations in the central Himalayas. *Geophys. Res. Lett.*, 2007, **34**, L23802.
11. Pandithurai, G., Dipu, S., Dani, K. K., Tiwari, S., Bisht, D. S., Devara, P. C. S. and Pinker, R. T., Aerosol radiative forcing during dust events over New Delhi, India. *J. Geophys. Res.*, 2008, **113**, D13209.
12. Liu, X. D. and Chen, B. D., Climatic warming in the Tibetan plateau during recent decades. *Int. J. Climatol.*, 2000, **20**, 1729–1742.
13. Dobhal, D. P. and Mehta, M., Surface morphology, elevation changes and terminus retreat of Dokriani Glacier, Garhwal Himalaya; implication for climate change. *Himalayan Geol.*, 2010, **31**(1), 71–78.
14. Ramanathan, V. *et al.*, Indian ocean experiment: an integrated analysis of the climate forcing and effects of the great Indo-Asian haze. *J. Geophys. Res.*, 2001, **106**, 28371–28398.
15. Lelieveld, J. *et al.*, The Indian Ocean experiment: widespread air pollution from South and Southeast Asia. *Science*, 2002, **291**, 1031–1036.
16. Tripathi, S. N., Dey, S., Tare, V. and Satheesh, S. K., Aerosol black carbon radiative forcing at an industrial city in northern India. *Geophys. Res. Lett.*, 2005, **32**, L08802.
17. Ganguly, D., Jayaraman, A., Rajesh, T. A. and Gadhavi, H., Wintertime aerosol properties during foggy and non foggy days over urban center Delhi and their implications for shortwave radiative forcing. *J. Geophys. Res.*, 2006, **111**, D15217.
18. Das, S. K., Jayaraman, A. and Misra, A., Fog-induced variations in aerosol optical and physical properties over the Indo-Gangetic Basin and impact to aerosol radiative forcing. *Ann. Geophys.*, 2008, **26**, 1345–1354.

19. Gergan, J. T., Dobhal, D. P. and Kaushik, R., Ground penetrating radar ice thickness measurements of Dokriani bamak (glacier), Garhwal Himalaya. *Curr. Sci.*, 1999, **77**, 169–174.
20. Dobhal, D. P. and Mehta, M., Snout fluctuation of Dokriani glacier (1962–2007) vis-à-vis the impact of climate change. *Himalayan Geol.*, 2008, **29**, 23–25.
21. Prasad, A. K., Singh, R. P. and Singh, A., Variability of aerosol optical depth over Indian subcontinent using MODIS data. *J. Indian Soc. Remote Sensing*, 2004, **32**, 313–316.
22. Satheesh, S. K. and Ramanathan, V., Large differences in tropical aerosol forcing at the top of the atmosphere and earth's surface. *Nature*, 2000, **405**, 60–63.
23. Kaufman, Y. J. *et al.*, Aerosol radiative impact on spectral solar flux at the surface, derived from principal-plane sky measurements. *J. Atmos. Sci.*, 2002, **59**, 635–646.
24. Deepshikha, S., Satheesh, S. K. and Srinivasan, J., Regional distribution of absorbing efficiency of dust aerosols over India and adjacent continents inferred using satellite remote sensing. *Geophys. Res. Lett.*, 2005, **32**, L03811.
25. Tanre, D., Kaufman, Y. J., Herman, M. and Mattoo, S., Remote sensing of aerosol properties over oceans using the MODIS/EOS spectral radiances. *J. Geophys. Res. D*, 1997, **102**(14), 16971–16988.
26. Remer, L. A. *et al.*, Validation of MODIS aerosol retrieval over ocean. *Geophys. Res. Lett.*, 2002, **29**, 1618.
27. Ricchiazzi, P., Yang, S., Gautier, C. and Sowle, D., SBDART, A research and teaching tool for plane-parallel radiative transfer in the earth's atmosphere. *Bull. Am. Meteorol. Soc.*, 1998, **79**, 2101–2114.
28. Ramana, M. V., Ramanathan, V., Podgorny, I. A., Pradhan, B. B., and Shrestha, B., The direct observations of large aerosol radiative forcing in the Himalayan region. *Geophys. Res. Lett.*, 2004, **31**, L05111.
29. Dumka, U. C., Satheesh, S. K., Pant, P., Hegde, P. and Moorthy, K. K., Surface changes in solar irradiance due to aerosols over central Himalayas. *Geophys. Res. Lett.*, 2006, **33**, L20809.
30. Hess, M., Keopke, P. and Schult, I., Optical properties of aerosols and clouds: the software package OPAC. *Bull. Am. Meteorol. Soc.*, 1998, **79**, 831–844.
31. Pant, P. *et al.*, Aerosol characteristics at a high-altitude location in central Himalayas: optical properties and radiative forcing. *J. Geophys. Res.*, 2006, **111**, D17206.
32. Vaughan, M. A., Winker, D. M. and Powell, K. A., CALIOP algorithm theoretical basis document, part 2: feature detection and layer properties algorithms. Report PC-SCI-202. NASA Langley Res. Cent., Hampton, Va, 2005, pp. 1–87.
33. Chand, D., Anderson, T. L., Wood, R., Charlson, R. J., Hu, Y., Liu, Z. and Vaughan, M., Quantifying above-cloud aerosol using space borne lidar for improved understanding of cloudy-sky direct climate forcing. *J. Geophys. Res.*, 2008, **113**, D13206.
34. Ganguly, D., Jayaraman, A. and Gadhavi, H., Physical and optical properties of aerosols over an urban location in western India: seasonal variabilities. *J. Geophys. Res.*, 2006, **111**, D24206.
35. Vuille, M., Bradley, R. S., Werner, M. and Keiming, F., 20th century climate change in the tropical Andes. *Climate Change*, 2003, **59**, 75–99.


ACKNOWLEDGEMENTS. The AOD data used in the present study were obtained from Goddard Earth Sciences Data and Information Services Center, USA. We thank the CALIPSO scientific team for providing free access to the data. We also thank the anonymous reviewer for useful comments that helped in improving the manuscript.

Received 6 January 2010; revised accepted 13 October 2010

# Sediment stratification and bathymetric survey using sediment echo sounder in reservoirs and shallow marine areas

**Girish Gopinath**

Centre for Water Resources Development and Management, Kozhikode 673 571, India

**The sediment echo sounder plays a pivotal role in assessing bathymetry as well as in the stratification of sediments in reservoirs and shallow marine areas. Reservoirs of India are facing reduction in capacity due to siltation process and this can be best quantified using the sediment echo sounder. The importance of this instrument is that it can establish water depths and identify significant sub-seabed reflectors and shallow stratigraphic units. The sediment echo sounder has also proved accurate and expeditious for reservoir desiltation studies as well as in shallow marine areas for developmental activities.**

**Keywords:** Bathymetry, reservoir desiltation, sediment echo sounder, sediment stratification.

STORAGE of water across rivers and construction of dams have been a strategy of mankind for survival for many centuries. Reservoirs play a vital role in irrigation, water supply, flood control and power generation. The siltation of reservoirs is a natural process, and it can be slowed down and controlled by a variety of soil conservation practices and modification of agricultural practices in the catchment areas. In case of desilting of reservoirs, issues relating to appropriate technology, various environmental aspects, and social and ecological problems are to be sorted out and resolved. The reservoir sedimentation status in India (and many other developing countries of the world) is disturbing. For example, sedimentation studies of the major 21 reservoirs in India have shown that the annual rate of siltation from the unit catchment is 40–2166% more than that assumed at the time when the project was designed[1]. Using the average of 21 reservoirs, the actual sedimentation inflow has been about 200% more than the design inflow. The sediment echo sounder can be used for studying sediment thickness as well as in the bathymetry of reservoirs and shallow marine areas. A significant application of this technology is in the volumetric calculation of different layers of sediments. For example, bathymetric and sedimentation surveys were conducted using a dual frequency (28/200 kHz) echo sounder system in two reservoirs (Lee Creek Reservoir and Lake Shepherd Springs) in the Ozark Plateau of northwestern Arkansas, USA[2]. Echo sounder survey data

e-mail: gg@cwrdm.org